Matsumoto, Junichi

Shape Identification for Navier-Stokes Equations Using Orthogonal Basis Bubble Function Finite Element Method

SHAPE IDENTIFICATION FOR NAVIER-STOKES EQUATIONS USING ORTHOGONAL BASIS BUBBLE FUNCTION FINITE ELEMENT METHOD

Junichi Matsumoto[1]

[1] Research Scientist, Advanced Manufacturing Research Institute (AMRI),
National Institute of Advanced Industrial Science and Technology (AIST),
1-2-1 Namiki,Tsukuba, Ibaraki 305-8564, Japan, e-mail: junmcct@ni.aist.go.jp

ABSTRACT

Numerical solutions for shape identification of flow past a circular cylinder are treated in this paper. The minimization algorithm based on Sakawa-Shindo method is employed. A unified computational approach to the simulation of flow and the shape identification with the shape smoothing is presented. As a numerical approach to spatial discretization, mixed interpolations by the improved bubble function and linear elements are applied for velocity and pressure.

Keywords: Navier-Stokes equations, shape optimization, shape smoothing, bubble function element stabilization method, orthogonal basis bubble function element

1. INTRODUCTION

A two-level three-level formulation of finite element method with bubble function is proposed for the incompressible Navier-Stokes equations (Matsumoto and Kawahara, 2001). Numerically, spatial discretization is applied to the mixed interpolation for the velocity and pressure fields by bubble element and linear element, respectively. Numerical solutions (Pironneau, 1973; Pironneau, 1974; Bourot, 1975; Ganesh, 1994; Azegami, 2000) for shape identification of flow past a circular cylinder are treated in this paper. The purpose of the study is to formulate and solve an analysis of shape identification for Navier-Stokes equations with unsteady flow. Generally, the state equations that govern incompressible viscous flow are written to include the Navier-Stokes equations. By described here in making the state equations a constraint of the performance function J, the Lagrange multiplier method is applied for shape identification (Matsumoto and Kawahara, 2001; Ogawa and Kawahara, 2003; Yagi and Kawahara, 2005; Shinohara *et al.*, 2008). To minimize the extended performance function J^*, it is necessary to solve the gradient of J^* with respect to the identified coordinates x_j. The necessary condition is that the stationary condition deriving from the first variation of J^* is set to zero. To improve the efficiency, stability, and accuracy of the calculation, the mixed interpolation that uses an orthogonal basis bubble function element stabilization method (Matsumoto, 2005) for the state equations of incompressible viscous fluid is applied. To validate the present method, the shape identification considered the smoothing technique of flow past a circular cylinder with periodic flow is analyzed. The identified drag force results in periodic solution region are similar to the objective results.

2. STATE EQUATION

The state equation that governs incompressible viscous flow is written as the following Navier-Stokes equation and the continuity equation in the non-dimensional form:

$$\dot{u}_i + u_j u_{i,j} + p_{,i} - \nu \left(u_{i,j} + u_{j,i}\right)_{,j} = 0 \quad in \quad \Omega \tag{1}$$

$$u_{i,i} = 0 \quad in \quad \Omega \tag{2}$$

u_i, p, and ν are the velocity, pressure, and the inverse of the Reynolds number, respectively. The boundary conditions are as follows:

$$u_i = \hat{u}_i \quad on \quad \Gamma_1 \tag{3}$$

$$\{-p\ \delta_{ij} + \nu \left(u_{i,j} + u_{j,i}\right)\} \cdot n_j = \hat{t}_i \quad on \quad \Gamma_2 \tag{4}$$

where the Dirichlet and the Neumann boundary conditions are specified on Γ_1 and Γ_2, respectively. Ω is the computational domain of $\mathbf{R}^2$. In equations (3) and (4), $\hat{u}_i$ denotes the values given on the boundary, n_j is the unit outward normal to Γ_2 and δ_{ij} are the Kronecker delta function. The initial condition of velocity at $t = t_0$ is specified on Ω,

$$u_{i(t_0)} = \hat{u}_{i0} \quad on \quad \Omega. \tag{5}$$

3. ORTHOGONAL BASIS BUBBLE FUNCTION ELEMENT STABILIZATION METHOD

3.1 Mixed interpolation

The MINI elements used in the spatial discretization of equations (1) and (2) is shown in Figure 1. The mixed interpolations for velocity and pressure are expressed as follows:

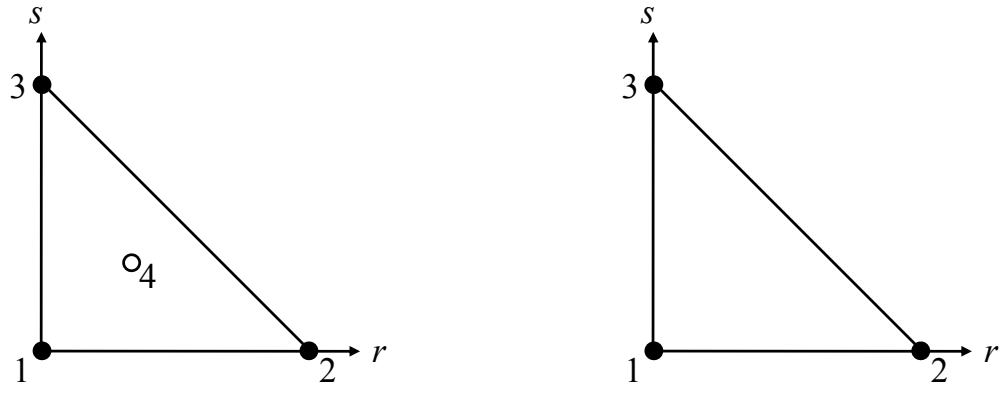

(a) Bubble function element (b) Linear element

Figure 1: Two-dimensional interpolation function.

$$u_i^h|_{\Omega_e} = \sum_{\alpha=1}^{3} \Phi_\alpha u_{\alpha i} + \phi_B u_{Bi},\ p^h|_{\Omega_e} = \sum_{\alpha=1}^{3} \Psi_\alpha p_\alpha,\ \Phi_\alpha = \Psi_\alpha - \frac{1}{3}\phi_B, \tag{6}$$

$$\Psi_1 = 1 - r - s,\ \Psi_2 = r,\ \Psi_3 = s. \tag{7}$$

Equation (6) is separated from the linear and bubble function interpolations as follows:

$$u_i^h|_{\Omega_e} = \bar{u}_i^h|_{\Omega_e} + u_i^{'h}|_{\Omega_e} \ , \ \bar{u}_i^h|_{\Omega_e} = \sum_{\alpha=1}^{3} \Psi_\alpha u_{\alpha i} \ , \ u_i^{'h}|_{\Omega_e} = \phi_B u_{Bi}^{'} \ , \ u_{Bi}^{'} = u_{Bi} - \frac{1}{3}\sum_{\alpha=1}^{3} u_{\alpha i}. \quad (8)$$

3.2 Bubble function element stabilization method

The two-level three-level finite element approximation (Matsumoto and Kawahara, 2001; Matsumoto, 2005) is considered to be a variation problem of finite element space with the bubble function element. In the two-level three-level finite element approximation, the two-level partition with a two-level bubble function is employed for determination of the finite element solution and the three-level partition with a three-level bubble function is applied to the weighting function. The piecewise linear finite element space $\bar{V}_i^h$, Q^h and the bubble function space $V_i^{h'}$, $\hat{V}_i^{h'}$ are defined by

$$\bar{V}_i^h = \{\bar{v}_i^h \in (H_0^1(\Omega))^2, \ \bar{v}_i^h|_{\Omega_e} \in (P1(\Omega_e))^2\}, \quad (9)$$

$$V_i^{h'} = \{v_i^{h'} \in (H_0^1(\Omega))^2, \ v_i^{h'}|_{\Omega_e} \in \phi_B v_{Bi}^{'}, \ v_{Bi}^{'} \in \mathbf{R}^2\}, \quad (10)$$

$$\hat{V}_i^{h'} = \{\hat{v}_i^{h'} \in (H_0^1(\Omega))^2, \ \hat{v}_i^{h'}|_{\Omega_e} \in \varphi_B v_{Bi}^{'}, \ v_{Bi}^{'} \in \mathbf{R}^2\}, \quad (11)$$

$$Q^h = \{q^h \in H_0^1(\Omega), \ q^h|_{\Omega_e} \in P1(\Omega_e), \ \int_\Omega q^h d\Omega = 0\}, \quad (12)$$

where ϕ_B and φ_B are the two- and three-level bubble functions with a compact support. In the approximation, the two- and three-level bubble functions are defined elementwise. The approximation is obtained by calculating the finite element solution $(u_i^h, p^h) \in V_i^h \times Q^h$, which is determined by the finite element space of $V_i^h = \bar{V}_i^h \oplus V_i^{'h}$ for the velocity field and Q^h for the pressure field,

$$\langle \dot{u}_i^h, \hat{v}_i^h \rangle + \langle \bar{u}_{0j}^h u_{i,j}^h, \hat{v}_i^h \rangle + \langle p_{,i}^h, \hat{v}_i^h \rangle - \langle \nu(u_{i,j}^h + u_{j,i}^h)_{,j}, \hat{v}_i^h \rangle = 0 \quad \forall \hat{v}_i^h \in \hat{V}_i^h, \quad (13)$$

$$\langle u_{i,i}^h, q^h \rangle = 0 \quad \forall q^h \in Q^h, \quad (14)$$

where

$$\langle u^h, v^h \rangle := \sum_{e=1}^{N_e} \langle u^h, v^h \rangle_{\Omega_e} := \sum_{e=1}^{N_e} \int_{\Omega_e} u^h v^h \ d\Omega \ , \ \bar{u}_{0j}^h|_{\Omega_e} := \frac{1}{A_e} \langle \bar{u}_j^h, 1 \rangle_{\Omega_e} \ , \ A_e := \int_{\Omega_e} d\Omega.$$

Here, $\langle \cdot, \cdot \rangle_{\Omega_e}$ denotes the L_2-inner product restricted to Ω_e, N_e is the number of elements, and $\bar{u}_{0j}^h$ is a constant defined elementwise by means of the velocity $\bar{u}_j^h$ by linear interpolation. The finite element solution u_i^h that belongs to V_i^h and the weighting function $\hat{v}_i^h$ that belongs to

$$\hat{V}_i^h = \bar{V}_i^h \oplus \{v_i^{h'} + \hat{v}_i^{h'}; \ v_i^{h'}|_{\Omega_e} + \hat{v}_i^{h'}|_{\Omega_e} = (\phi_B + \varphi_B) v_{Bi}^{'}\}$$

can be expressed as follows:

$$u_i^h = \bar{u}_i^h + u_i^{h'} \ , \ \hat{v}_i^h = \bar{v}_i^h + v_i^{h'} + \hat{v}_i^{h'} = v_i^h + \hat{v}_i^{h'}, \quad (15)$$

where

$$\bar{u}_i^h, \ \bar{v}_i^h \in \bar{V}_i^h \ , \ u_i^{'h} = \sum_{e=1}^{N_e} \phi_B u_{Bi}^{'} \in V_i^{'h} \ ,$$

$$v_i^{'h} = \sum_{e=1}^{N_e} \phi_B v_{Bi}^{'} \in V_i^{'h} \ , \ \hat{v}_i^{'h} = \sum_{e=1}^{N_e} \varphi_B v_{Bi}^{'} \in \hat{V}_i^{'h}. \tag{16}$$

The two-level bubble function is used the orthogonal basis bubble function element (Matsumoto, 2005) for P1B element. The orthogonal basis bubble function element has the following relation equation (17).

$$\langle \phi_B, 1 \rangle_{\Omega_e} = \langle \phi_B^2, 1 \rangle_{\Omega_e} = \frac{N+1}{N+2} A_e. \tag{17}$$

N is space dimension number. It is assumed that the three-level bubble function satisfies the following equations:

$$\langle \Psi_\alpha, \varphi_B \rangle_{\Omega_e} = \frac{1}{N+1} \langle 1, \varphi_B \rangle_{\Omega_e} \ , \ \alpha = 1 \cdots N+1, \tag{18}$$

$$\langle 1, \varphi_B \rangle_{\Omega_e} = 0 \ , \ \langle \phi_B, \varphi_B \rangle_{\Omega_e} = 0. \tag{19}$$

The finite element equations that are employed in the bubble function element stabilization method are given as follows:

$$\langle \dot{u}_i^h, v_i^h \rangle + \langle \bar{u}_{0j}^h u_{i,j}^h, v_i^h \rangle - \langle p^h, v_{i,i}^h \rangle + \langle \nu (\bar{u}_{i,j}^h + \bar{u}_{j,i}^h), \bar{v}_{i,j}^h \rangle$$

$$+ \sum_{e=1}^{N_e} \langle (\nu + \nu_i^{'})(u_{i,j}^{h'} + u_{j,i}^{h'}), v_{i,j}^{h'} \rangle_{\Omega_e} = \langle t_i, v_i^h \rangle_\Gamma \quad \forall v_i^h \in V_i^h, \tag{20}$$

$$\langle u_{i,i}^h, q^h \rangle = 0 \quad \forall q^h \in Q^h, \tag{21}$$

$$\nu_i^{'} := \langle \dot{u}_i^h + \bar{u}_{0j}^h u_{i,j}^h + p_{,i}^h - \nu (u_{i,j}^h + u_{j,i}^h)_{,j}, \varphi_B \rangle_{\Omega_e} \Big/ \langle (u_{i,j}^{h'} + u_{j,i}^{h'}), \phi_{B,j} \rangle_{\Omega_e}.$$

The stabilized operator control term $\sum_{e=1}^{N_e} \langle \nu_i^{'} (u_{i,j}^{h'} + u_{j,i}^{h'}), v_{i,j}^{h'} \rangle_{\Omega_e}$ is derived from the three-level bubble function. The stabilized operator control parameter $\nu_i^{'}$ can be determined as follows (Matsumoto and Kawahara, 2001; Matsumoto, 2005) :

$$\langle (\nu + \nu_i^{'})(u_{i,j}^{h'} + u_{j,i}^{h'}), v_{i,j}^{h'} \rangle_{\Omega_e} = \frac{\langle \phi_B, 1 \rangle_{\Omega_e}^2}{A_e} \tau_{eR}^{-1} \delta_{ij} u_{Bi}^{'} v_{Bi}^{'}, \tag{22}$$

$$\tau_{eR} = \left[\left(\frac{2|u_i|}{h_e} \right)^2 + \left(\frac{4\nu}{h_e^2} \right)^2 \right]^{-\frac{1}{2}}.$$

h_e is the element length (Tezduyar and Osawa, 2000).

4. PERFORMANCE FUNCTION

Finite element equations (20) and (21) can be described as follows:

$$v_i^T (M \dot{u}_i + S(\bar{u}_{0j}) u_i - Bp - M_\Gamma t_i) = 0 \quad in \quad \Omega, \tag{23}$$

$$q^T (B^T u_i) = 0 \quad in \quad \Omega, \tag{24}$$

$$u_{i(t_0)} = \hat{u}_{i0} \quad on \quad \Omega. \tag{25}$$

Shape identification formulates the problem that performance function is defined as follows:

$$J = \frac{1}{2}\int_{t_0}^{t_f}(e_{\Gamma_B}^T M_\Gamma t_i - D_i)^T Q_i (e_{\Gamma_B}^T M_\Gamma t_i - D_i)dt + \frac{1}{2}\int_{t_0}^{t_f}(A_C - A_0)Q_a(A_C - A_0)\ dt, \quad (26)$$

where

$$e_{\Gamma_B}^T M_\Gamma t_i = -\int_{\Gamma_B} t_i d\Gamma\ ,\ e_{\Gamma_B}^T = [0,0,0,-1,-1,-1,\ldots,0,0,0]. \quad (27)$$

Q_i is 1 and Q_a is defined by the following equation (28).

$$Q_a = \int_{t_0}^{t_f}(e_{\Gamma_B}^T M_\Gamma t_i - D_i)^{T(0)} Q_i (e_{\Gamma_B}^T M_\Gamma t_i - D_i)^{(0)} dt \Big/ \int_{t_0}^{t_f} A_C^{2(0)}\ dt. \quad (28)$$

t_i, Q_i and D_i are traction value, weighting parameter and objective value, respectively. A_C and A_0 are a computed area of identified shape and objective area. By making the state equation a constraint of the performance function J, the Lagrange multiplier method was applied for shape identification. The Lagrange multipliers for the equation are defined as the adjoint velocity λ_{u_i} and pressure λ_p to introduce them. The extended performance function J^* can be defined as follows:

$$J^* = J + \int_{t_0}^{t_f}\lambda_{u_i}^T(-S(\bar{u}_{0j})u_i + Bp + M_\Gamma t_i - M\dot{u}_i)\ dt + \int_{t_0}^{t_f}\lambda_p^T(B^T u_i)\ dt. \quad (29)$$

5. ADJOINT EQUATION

To minimize the extended performance function J^*, it is necessary to solve the gradient of J^* with respect to the identified coordinates x_j. The necessary condition is that the stationary condition deriving from the first variation of J^* is set to zero, that is,

$$\delta J^* = 0, \quad (30)$$

then, the adjoint state equation terminal condition to be solved can be obtained as follows:

$$M\dot{\lambda}_{u_i} - \tilde{S}(u_j)^T\lambda_{u_i} + B\lambda_p = 0 \quad in \quad \Omega, \quad (31)$$

$$B^T\lambda_{u_i} = 0 \quad in \quad \Omega, \quad (32)$$

$$\lambda_{u_{i(t_f)}} = 0 \quad in \quad \Omega, \quad (33)$$

$$\lambda_{u_i} = -e_{\Gamma_B}Q_i(e_{\Gamma_B}^T M_\Gamma t_i - D_i) \quad on \quad \Gamma. \quad (34)$$

6. TIME DISCRETIZATION

6.1 Time discretization of the state equation

To discretize the state equation, a quasi-linear form is given by

$$M\frac{u_i^{n+1} - u_i^n}{\Delta t} + S(\bar{u}_{0j}^*)u_i^{n+1/2} - Bp^{n+1} = M_L t_i, \quad (35)$$

$$B^T u_i^{n+1} = 0, \tag{36}$$

where

$$u_j^* = \frac{1}{2}(3u_j^n - u_j^{n-1}) \ , \ u_i^{n+1/2} = \frac{1}{2}(u_i^{n+1} + u_i^n),$$

is employed. To discretize the quasi-linear form in time, the second-order linear time integrator was used. The boundary value problem is given by

$$M\frac{\tilde{u}_i^{n+1} - u_i^n}{\Delta t} + S(\bar{u}_{0j}^*)\tilde{u}_i^{n+1/2} - Bp^n = M_L t_i, \tag{37}$$

$$B^T \bar{M}^{-1} B\Delta t(p^{n+1} - p^n) = -B^T \tilde{u}_i^{n+1}, \tag{38}$$

$$M\frac{u_i^{n+1} - \tilde{u}_i^{n+1}}{\Delta t} + \frac{1}{2}S(u_j^*)(u_i^{n+1} - \tilde{u}_i^{n+1}) - B(p^{n+1} - p^n) = 0, \tag{39}$$

where

$$\tilde{u}_i^{n+1/2} = \frac{1}{2}(\tilde{u}_i^{n+1} + u_i^n)$$

is finally derived. M is the mass matrix, and $S(\bar{u}_{0j}^*)$ is the matrix of the advection term and viscosity term. B is the gradient matrix, and $M_L t_i$ is boundary integration term. An important point to be noted is that the consistent mass matrix M is a diagonal matrix on account of the orthogonal intersection of the basis functions of the orthogonal basis bubble function element.

6.2 Time discretization of the adjoint equation

To discretize the quasi-linear form in time, the second-order linear time integrator is used. The boundary value problem is given by

$$M\frac{\tilde{\lambda}_{u_i}^{n-1} - \lambda {u_i}^n}{\Delta t} + \tilde{S}(\bar{u}_{0j}^*)^T \tilde{\lambda}_{u_i}^{n-1/2} - B\lambda p^n = 0, \tag{40}$$

$$B^T M^{-1} B\Delta t(\lambda_p^{n-1} - \lambda_p^n) = -B^T \tilde{\lambda}_{u_i}^{n-1}, \tag{41}$$

$$M\frac{\lambda_{u_i}^{n-1} - \tilde{\lambda}_{u_i}^{n-1}}{\Delta t} + \frac{1}{2}\tilde{S}(\bar{u}_{0j}^*)^T(\lambda {u_i}^{n-1} - \tilde{\lambda}_{u_i}^{n-1}) - B(\lambda_p^{n-1} - \lambda_p^n) = 0, \tag{42}$$

where

$$\tilde{\lambda}_{u_i}^{n-1/2} = \frac{1}{2}(\tilde{\lambda}_{u_i}^{n-1} + \lambda_{u_i}^n),$$

is finally derived. $\tilde{S}(\bar{u}_{0j})^T$ is the transposed matrix of the linearlized $S(\bar{u}_{0j})u$

7. MINIMIZATION ALGORITHM WITH SHAPE SMOOTHING

The minimization algorithm based on Sakawa-Shindo method (Sakawa and Shindo, 1980) is used. The identified coordinate values are renewed by the following equation,

$$x_j^{(l+1)} = x_j^{(l)} + \alpha^{(l)}\tilde{d}_j^{(l)}. \tag{43}$$

(l) is the iteration step, and $\alpha^{(l)}$ is the weighting coefficient. $\alpha^{(l)}$ is renewed with every iteration. $\tilde{d}_j^{(l)}$ is the value that is smoothed by the following equations (44) and (45) of $d_j^{(l)}$.

- Iterate: For m = 1,2,. . .,m_s do.

$$\bar{M}_s \; \tilde{d}_j^{(l)} = \tilde{M}_s \; d_j^{(l)} \quad on \quad \Gamma_B, \tag{44}$$

$$\tilde{d}_j^{(l)} \longrightarrow d_j^{(l)}. \tag{45}$$

This is called the selective lumping method (Kawahara and Hirano, 1983). Here,

$$\tilde{M}_s = e_s \bar{M}_s + (1 - e_s) M_s \; , \; 0 \leq e_s \leq 1, \tag{46}$$

$$d_j^{(l)} = -\int_{t_0}^{t_f} \left\{ \lambda_{u_i}^T \left[-\left\{ \frac{\partial S(\bar{u}_j)}{\partial x_j^{(l)}} \right\} u_i + \left\{ \frac{\partial B}{\partial x_j^{(l)}} \right\} p \right] \right.$$
$$\left. + \lambda_p^T \left\{ \frac{\partial B^T}{\partial x_j^{(l)}} \right\} u_i + \left\{ \frac{\partial A_C}{\partial x_j^{(l)}} \right\} Q_a (A_C - A_0) \right\}^{T(l)} dt. \tag{47}$$

$\bar{M}_s$ and M_s are lumped and consistent mass matrices on surface element of identified shape. e_s is lumping parameter. The calculation algorithm based on Sakawa-Shindo method is summarized as follows:

1. Set $l = 0$ and assume the initial identified vector $x_j^{(l)}$.
2. Solve the initial state vector $u_i^{(l)}$, $p^{(l)}$ using equations (37)-(39).
3. Solve the initial performance function $J^{(l)}$ using equation (26).
4. Solve the Lagrangian multiplier vector $\lambda_{u_i}^{(l)}$, $\lambda_p^{(l)}$ using equations (40)-(42).
5. Solve the identified vector $x_j^{(l+1)}$ using equation (43).
6. Solve the error norm $e = ||x_j^{(l+1)} - x_j^{(l)}||_\infty$, and if $e < \varepsilon$ then stop, else go to 7.
7. Solve the state vector $u_i^{(l+1)}$, $p^{(l+1)}$ using equations (37)-(39).
8. Solve the performance function $J^{(l+1)}$ using equation (26).
9. The weighting parameter $\alpha^{(l)}$ is changed as follows: If $J^{(l+1)} \leq J^{(l)}$ then $\alpha^{(l+1)} = \frac{10}{9}\alpha^{(l)}$ and go to 4., else $\alpha^{(l)} = \frac{1}{2}\alpha^{(l)}$ and go to 5.

In the algorithm, $\alpha^{(0)}$ is decided by $\alpha^{(0)} = \Delta\hat{x}_j \; / \; \left\| \tilde{d}_j^{(0)} \right\|_\infty$.

8. NUMERICAL RESULTS FOR FLOW PAST A CIRCULAR CYLINDER

8.1 Flow past a circular cylinder

To validate the present method, the shape identification with the smoothing technique of flow past a circular cylinder is analyzed. The computational domain shown in Figure is 12 D wide and 24 D long. The central point of the circular cylinder is located to the position in 6D width and 6D length. The initial finite element mesh is shown in Figure 3. The total numbers of nodes and elements are 1834 and 3500, respectively.

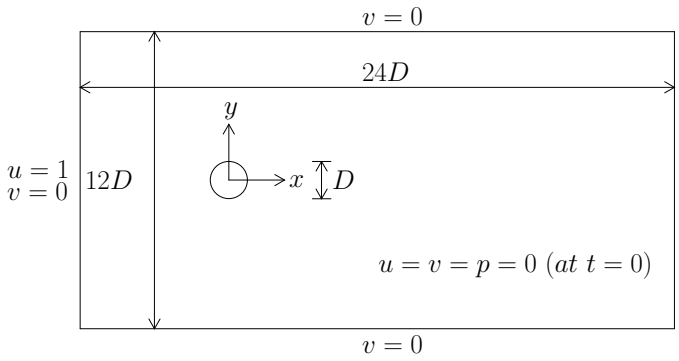

Figure 2: Computational domain.

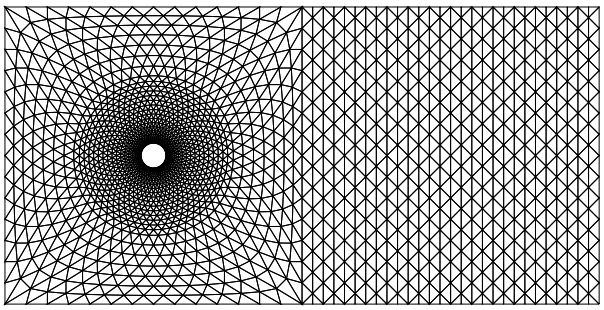

Figure 3: Initial finite element mesh.

8.2 Shape optimization

Two shape optimization problems for the incompressible Navier-Stokes equations are investigated. One , case1, is a drag force minimization with area constant of identified shape. The other, case2, is a drag force constant with internal area maximization of identified shape. Case1 is defined by equation (48).

$$J = \frac{1}{2}\int_{t_0}^{t_f} (e_{\Gamma_B}^T M_\Gamma t_1)^T Q_1 (e_{\Gamma_B}^T M_\Gamma t_1) dt + \frac{1}{2}\int_{t_0}^{t_f} (A_C - A_0) Q_a (A_C - A_0)\ dt \qquad (48)$$

A_C is the computed external area of identified shape. A_0 is the computed external area of initial shape. Case2 is defined by equation (49).

$$J = \frac{1}{2}\int_{t_0}^{t_f} (e_{\Gamma_B}^T M_\Gamma t_1 - D_1)^T Q_1 (e_{\Gamma_B}^T M_\Gamma t_1 - D_1) dt + \frac{1}{2}\int_{t_0}^{t_f} A_C Q_a A_C\ dt \qquad (49)$$

D_1 is the drag force that was obtained by case1. The optimal shape is comparison between the result of case1 and the result of case2.

8.3 Shape smoothing

The effect of shape smoothing by selective lumping method is examined. The results of shape smoothing in the shape optimization problem of case1 are shown in figure 4. The numerical results are used Δt=0.2 and $\Delta \hat{x}_j$=0.01. Dotted line means the initial shape. Solid line means the identified shape. As for (a), (b), and (c) the identified shapes are sharp, because the effect of smoothing is not working. On the other hand, as for (d), (e),

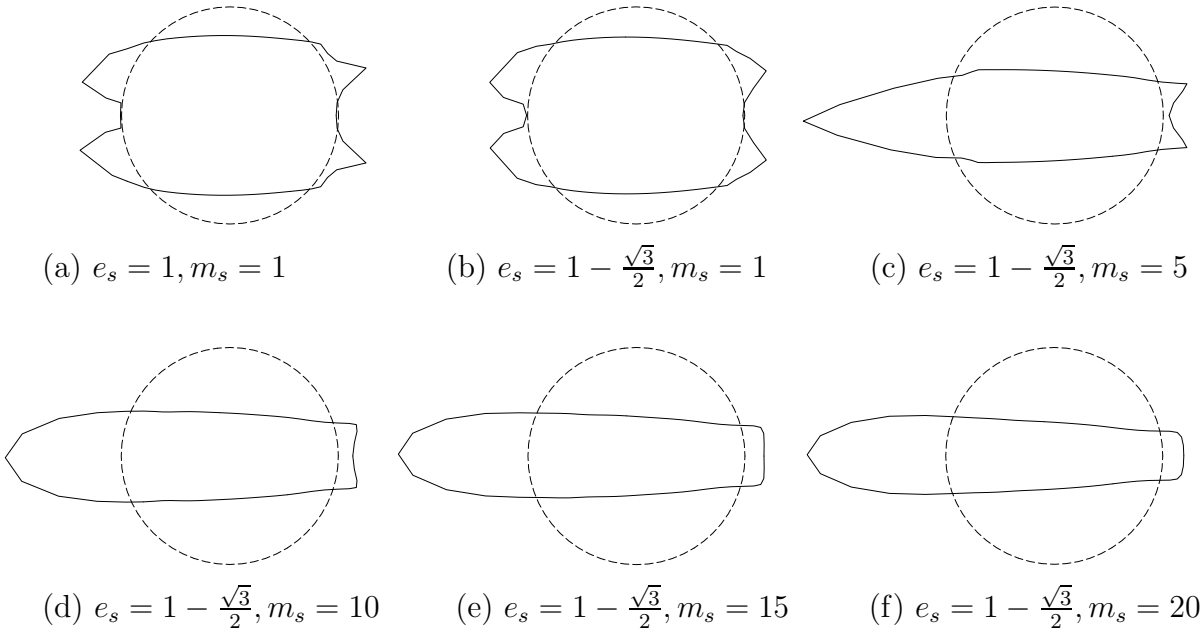

(a) $e_s = 1, m_s = 1$ (b) $e_s = 1 - \frac{\sqrt{3}}{2}, m_s = 1$ (c) $e_s = 1 - \frac{\sqrt{3}}{2}, m_s = 5$

(d) $e_s = 1 - \frac{\sqrt{3}}{2}, m_s = 10$ (e) $e_s = 1 - \frac{\sqrt{3}}{2}, m_s = 15$ (f) $e_s = 1 - \frac{\sqrt{3}}{2}, m_s = 20$

Figure 4: Shape smoothing in the shape optimization problem of case1. (Re=250)

and (f) the identified shapes are smooth, because the effect of smoothing is working.

8.4 Numerical results

The results of shape optimization are shown in Figures 5. The numerical results are used Δt=0.2 and $\Delta \hat{x}_j$=0.01. The identified shape (a) is similar to the identified shape (b).

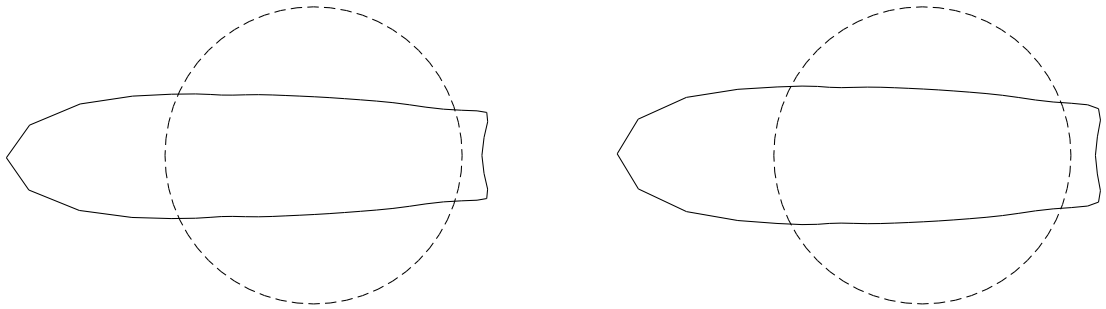

(a) Case1 (b) Case2

Figure 5: Numerical results of shape optimization. ($e_s = 1 - \frac{\sqrt{3}}{2}, m_s = 10$, Re=250)

9. CONCLUSIONS

In this study, the numerical solutions for the two shape optimizations of flow past a circular cylinder were analyzed. The minimization algorithm based on Sakawa-Shindo method is proposed. A unified computational approach to the simulation of flow and the shape identification with the smoothing technique was presented. As a numerical approach for spatial discretization, that mixed interpolation by bubble and linear elements was applied

for velocity, and that by a linear element was applied for pressure. The present results obtained in the incompressible Navier-Stokes equations, the identified shape of a drag force minimization with area constant is similar to the identified shape of a drag force constant with internal area maximization.

REFERENCES

Matsumoto, J. and Kawahara, M. (2001), Shape identification for fluid-structure interaction problem using improved bubble element, *Int. J. Comput. Fluid Dyn.*, 15, pp.33-45.

Pironneau, O. (1973), On optimum profiles in Stokes flow, *J. Fluid Mech.*, 59, Part1, pp.117-128.

Pironneau, O. (1974), On optimum design in fluid mechanics, *J. Fluid Mech.*, 64, Part 1, pp.97-110.

Bourot, J.M. (1975), On the numerical computation of the optimum profile in Stokes flow, *J. Fluid Mech.*, 65, Part 3, pp.513.

Ganesh, R.K. (1994), The minimun drag profile in laminar flow: a numerical, *Transaction of the ASME, J. Fluids Engng.*, 116, pp.456-462.

Azegami, H. (2000), Solution to boundary shape identification problem in elliptic boundary value problem using shape derivatives, *Inverse Problems in Engineering Mechanics II*, pp.277-284.

Ogawa, Y. and Kawahara, M. (2003), Shape optimization of body located in incompressible viscous flow based on optimal control theory, *Int. J. Comput. Fluid Dyn.*, 17, pp.243-251.

Yagi, H. and Kawahara, M. (2005), Shape optimization of a body located in low Reynolds, *Int. J. Numer. Meth. Fluids*, 48, pp.819-833.

Shinohara, K., Okuda, H., Ito, S., Nakajima, N., and Ida, M. (2008), Shape optimization using adjoint variable method for reducing drag in Stokes flow, *Int. J. Numer. Meth. Fluids*, Published online.

Matsumoto, J. (2005), A relationship between stabilized FEM and bubble function element stabilization method with orthogonal basis for incompressible flows, *J. Appl. Mech., JSCE*, 8, pp.233-242.

Tezduyar, T.E. and Osawa, Y. (2000), Finite element stabilization parameters computed from element matrices and vectors, *Comput. Method Appl. Mech. Engrg.*, 190, pp.411-430.

Sakawa, Y. and Shindo, Y. (1980), On global convergence of an algorithm for optimal control, *Transactions on Automatic Control, IEEE*, AC-25(6), pp.1149-1153.

Kawahara, M. and Hirano, H. (1983), Two step explicit finite element method for high Reynolds number viscous fluid flow, *Proc. of JSCE*, 329.